The study of the influence of the geometry of the double legged ducts on the buildup factor and the transmitted flux

Z. Faik Ouahab

Faculté des Sciences Semlalia, BP 2390,Université Caddy Ayyad, Marrakech
e-mail : fozakaria@hotmail.com

Received 27 November 2023; accepted 12 March 2025

The analysis of neutron transport through ducts holds significant importance due to its applicability in numerous practical scenarios, particularly in systems involving complex duct geometries. The presence of these ducts is inevitable in several nuclear installations. In this work, we have developed a simulation program based on the Monte Carlo method that has been validated by the MCNPX calculation code. We have also introduced a new concept of buildup factor in order to study the effect of the geometry of the double legged duct on the buildup factor and the flux at the duct exit.

Keywords: Monte Carlo; neutrons; duct; buildup factor; transmission flux.

DOI: https://doi.org/10.31349/RevMexFis.71.051201

1. Introduction

The transport of neutrons in bent ducts has been the subject of several works based on the simulation by the Monte Carlo method [1-5]. These studies are based on the phenomena of neutron flow and reflection which become annoying when the number of bends increases. The study of the radiation flow through bent ducts has been the subject of several studies in order to find simplified calculation methods to solve this problem with analytical solutions [6-14].

The buildup factor is a factor that makes it possible to take into account the scattered particles in the calculations carried out by the straight-line attenuation method. It depends on the energy of the incident particles, the nature and the thickness of the traversed materials. In this study, we consider a full bent aluminum duct surrounded by iron and we have developed a program based on Monte Carlo simulation and a new concept of buildup factor [15] that we will apply to calculate the transmitted flux and the neutron buildup factor according to different incident neutron energies, different sections of the bent duct and different lengths.

2. Method principle

To establish a new concept of the neutron accumulation factor in a bent duct, we considered a direct attenuation of the neutron in the legs and then an imposed diffusion of $\theta = \pi/2$ at each surface (S1 and S2) joining the outer corners of the duct (Fig. 1). The presence of two 90° bends significantly influences neutron scattering and absorption, impacting the overall transmission through the duct.

The duct consists of three legs, with neutron transport analyzed in Area 1 and Area 2, where the effects of scattering and attenuation after each bent are examined. A neutron source, characterized by energy and intensity, is injected at the entry of the duct. The neutron source is assumed to have an isotropic angular distribution, ensuring uniform emission in all directions. The initial neutron density follows a homogeneous distribution across the cross-section of the duct's entry, allowing for an even probability of neutron interactions within the duct structure. The transmitted flux at the exit is evaluated as a function of the incident neutron energy and the duct's geometric parameters.

We have developed a simulation program based on the Monte Carlo method that we have validated by the MCNPX calculation code [16] and an expression of the flow at the output of the bent duct as follows [15]:

$$\Phi = P^2\left(\frac{\pi}{2}\right) P_{S_1} P_{S_2} \sinh(\Sigma_1 a) \sinh(\Sigma_3 a) \frac{1}{\Sigma_1 \Sigma_3 a^4 4\sqrt{2}} \times \exp -(\Sigma_1 h_1 + \Sigma_2 h_2 + \Sigma_3 h_3 + 2a\Sigma_2), \quad (1)$$

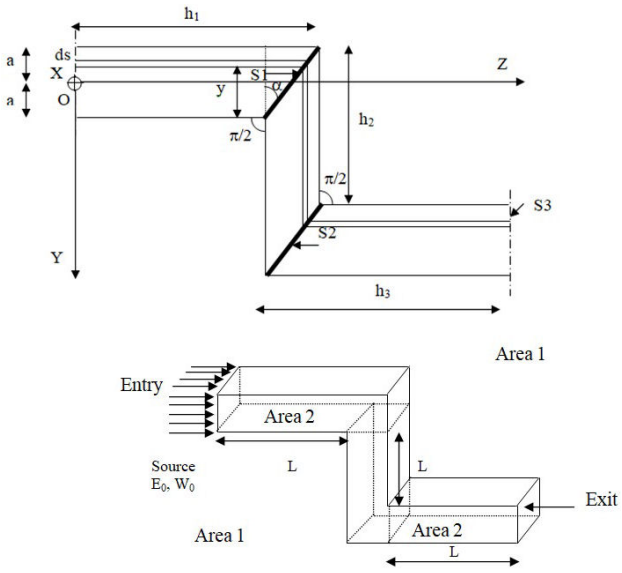

FIGURE 1. Geometrical configuration and neutron transport in a bent duct.

Σ_1, Σ_2 and Σ_3 are the total macroscopic cross-sections of the neutron in the first, second and third legs. h_1, h_2 and h_3 are the lengths of the 1st, 2nd and 3rd leg. a is the half of the duct square section side. P_{S_1} and P_{S_2} are the probabilities of diffusion at the 1st bend and at the 2nd bend.

Under real attenuation conditions, the interactions of neutrons with the material are not pure absorptions. The flux at a point must take into account the neutrons that have undergone diffusions in the area and have lost part of their energy. The flow given by Eq. (1) has replaced the flow without collision in homogeneous environments to calculate the buildup factor [17-18]. The new buildup factor that we have proposed is given by the ratio of the total flux transmitted at the output of the duct determined by the Monte Carlo simulation (Φ_{SMC}) on the flux given by Eq. (1)

$$\text{Buildup factor} = \frac{\Phi_{SMC}}{\Phi}. \tag{2}$$

3. Results and discussions

From the flux formula represented above in Eq. (1), we have calculated the flux leaving a bent duct, filled with aluminum according to the energy of the incident neutrons for different lengths of the legs of the duct (the legs are equal in length L) and different sides of the square section.

Figures 2 and 3 illustrate the neutron flux transmission through the bent duct as a function of neutron energy for different duct lengths and different sides of the square section. Several dips are observed in the flux distribution, which are associated with energy-dependent interactions between neutrons and the duct material. In particular, a pronounced dip around $E = 35$ keV is attributed to resonance absorption phenomena in aluminum (Fig. 4). This effect arises due to the sharp increase in the total macroscopic cross-section of aluminum in this energy range, leading to significant neutron absorption and reduced transmitted flux. The resonance behavior observed at 35 keV is predominantly caused by neutron interactions with aluminum nuclei, specifically due to

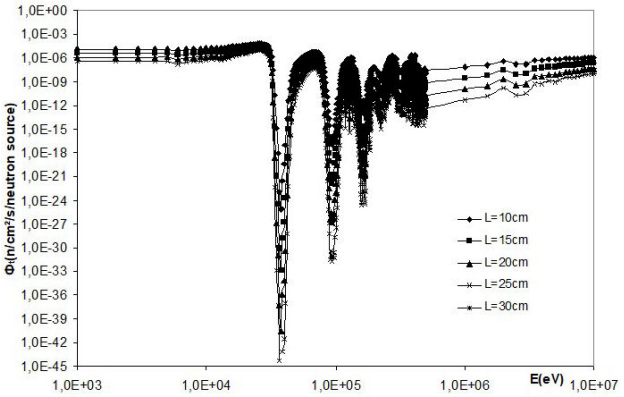

FIGURE 2. The neutron flux at the outlet of the aluminum duct according to the energy of the incident neutrons for a duct with a square cross section of 64 cm^2 and for different lengths of the legs.

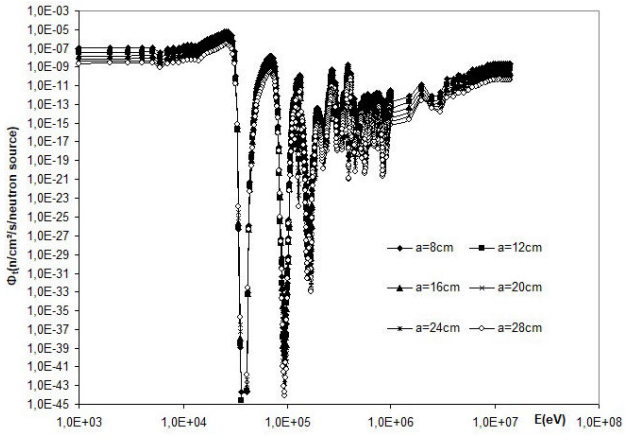

FIGURE 3. The neutron flux at the outlet of the aluminum duct according to the energy of the incident neutrons for a duct with a leg length $L = 30$ cm and for different square sections of the duct.

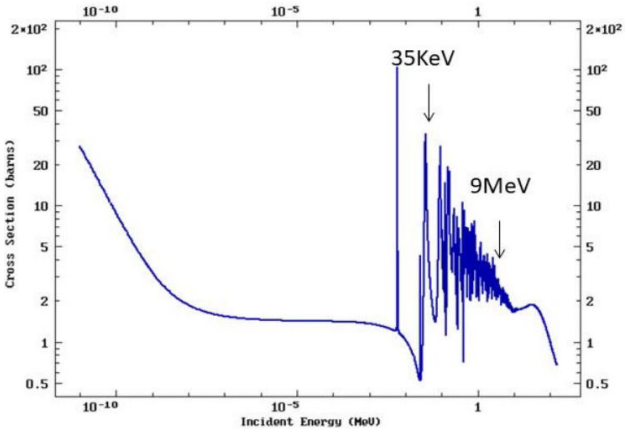

FIGURE 4. Total cross-section variation as a function of energy for aluminum-27 according to database ENDF/B-VIII.0

radiative capture (n, γ) reactions. At this energy, aluminum exhibits enhanced neutron capture probabilities due to the formation of compound nuclear states, temporarily trapping the neutron before releasing energy in the form of gamma radiation. This phenomenon is well-documented in neutron cross-section databases such as ENDF/B-VIII.0 and has been studied extensively in neutron shielding and reactor design applications. Figure 5 illustrates the evolution of neutron flux as a function of distance L for three different materials: aluminum (Al), iron (F_e), and hydrogen (H). The graph shows a decrease in neutron flux with increasing distance, which is consistent with neutron attenuation through matter. The rate of decline varies depending on the material: iron exhibits the most significant attenuation, followed by hydrogen, while aluminum shows the slowest decrease. This trend is expected since iron, due to its high atomic number and larger interaction cross-section, absorbs and scatters neutrons more effectively than hydrogen and aluminum.

In the case where the duct is surrounded by iron, this factor increases according to the length of the duct; it decreases when the energy of the incident neutrons increases and its

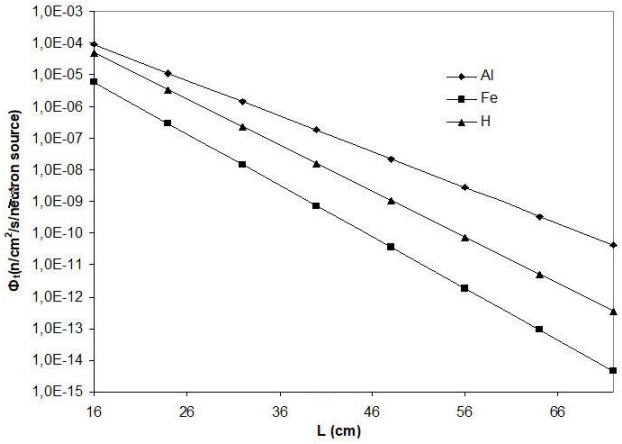

FIGURE 5. Variation of the flux according to the length of the duct for a square cross-section of 64 cm^2 and an energy of 2 MeV for different materials.

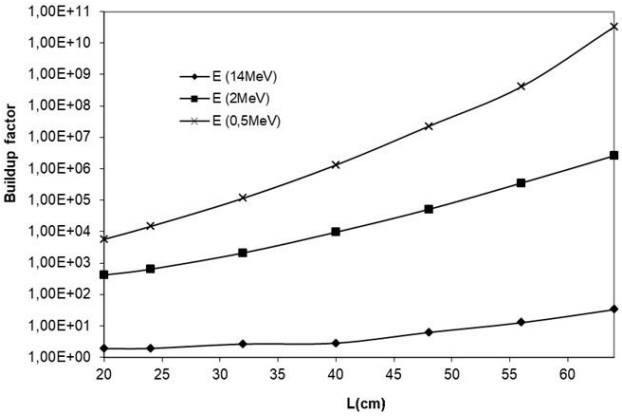

FIGURE 6. The buildup factor according to the length of the bent duct for different energy values and for a square cross-section of 64 cm^2.

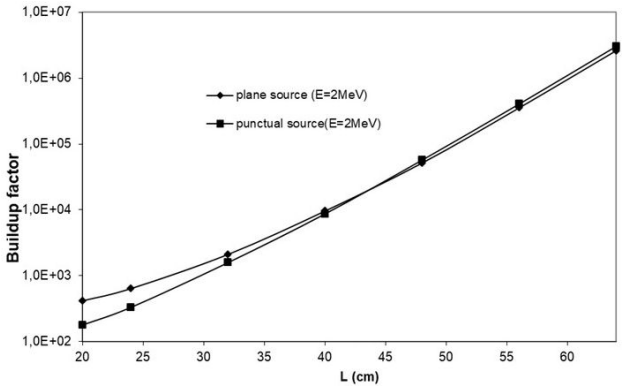

FIGURE 7. The buildup factor according to the length of the bent duct for different sources and for a square section of 64 cm^2.

value is greater than 1 because of the reflections on the walls, the thing that increases the transmitted flux (Fig. 6). We can also deduce from Fig. 7 that the buildup factor is greater at a short length of the duct when the radiation source is plane, whereas the point source prevails for long distances. Figures 8 to 11 show the variations in the neutron flux as according to the neutron energy for different lengths of the legs and different sides of the bent duct. In a bent aluminum duct, the

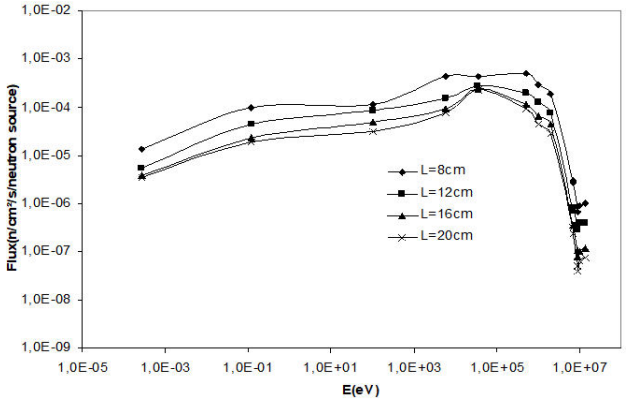

FIGURE 8. Neutron flux according to the energy for different lengths of the legs of the duct (the side of the square section is $a = 8$ cm).

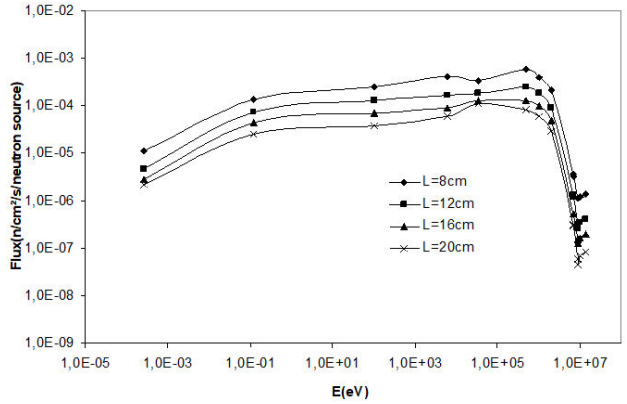

FIGURE 9. Neutron flux according to the energy for different lengths of the legs of the duct (the side of the square section is $a = 12$ cm).

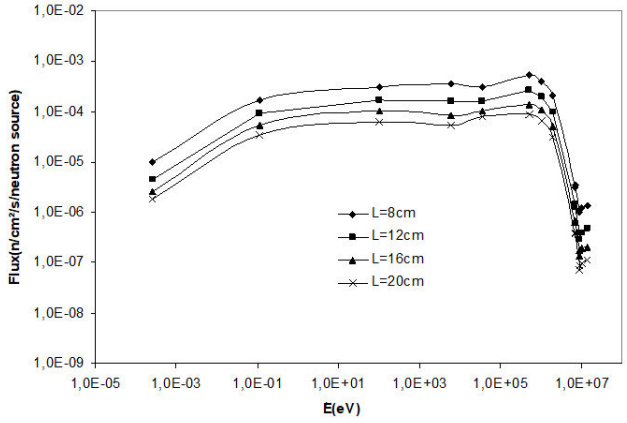

FIGURE 10. Neutron flux according to the energy for different lengths of the legs of the duct (the side of the square section is $a = 16$ cm).

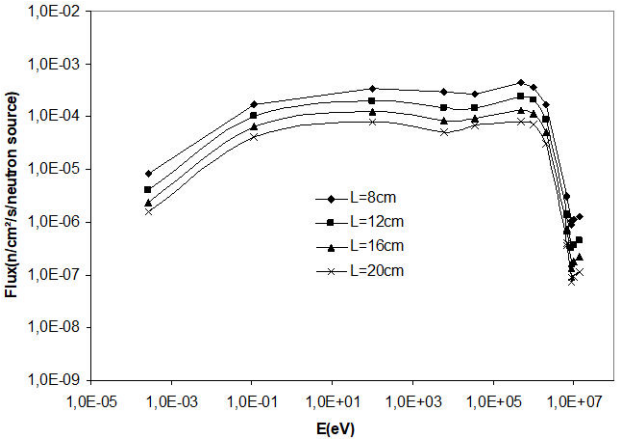

FIGURE 11. Neutron flux according to the energy for different lengths of the legs of the duct (the side of the square section is $a = 20$ cm).

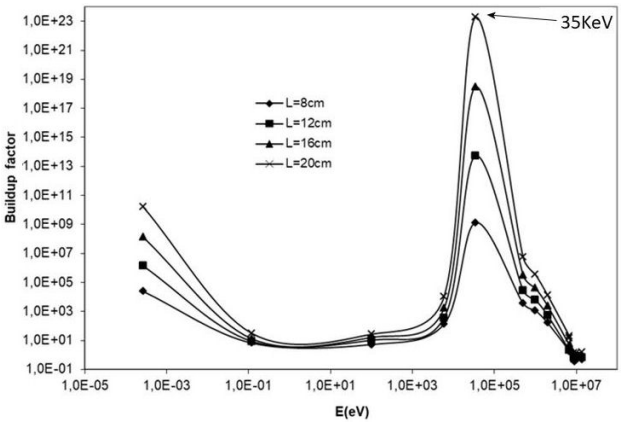

FIGURE 12. The buildup factor according to the energy of the incident neutrons for different lengths of the legs and for a square cross-section of 64 cm^2.

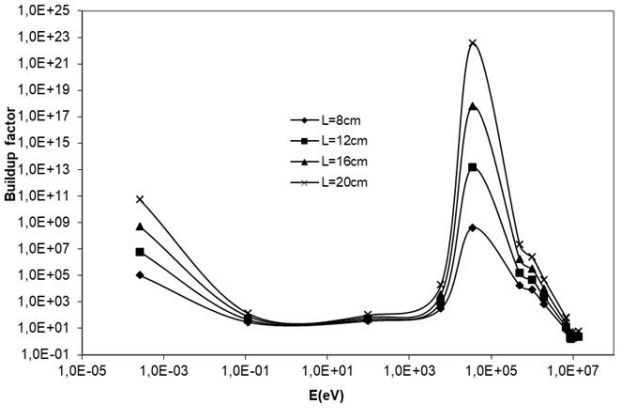

FIGURE 13. The buildup factor according to the energy of the incident neutrons for different lengths of the legs and for a square cross-section of 144 cm^2.

reduction in high-energy neutron flux results from several interconnected physical phenomena. Fast neutrons undergo elastic scattering with aluminum nuclei, leading to a loss of energy. As they pass through the bent, their trajectory

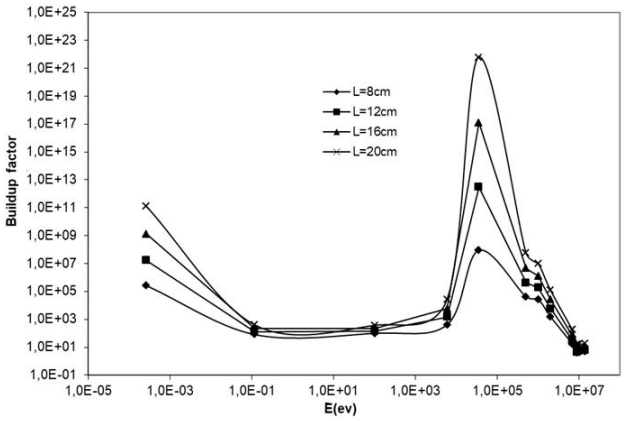

FIGURE 14. The buildup factor according to the energy of the incident neutrons for different lengths of the legs and for a square cross-section of 256 cm^2.

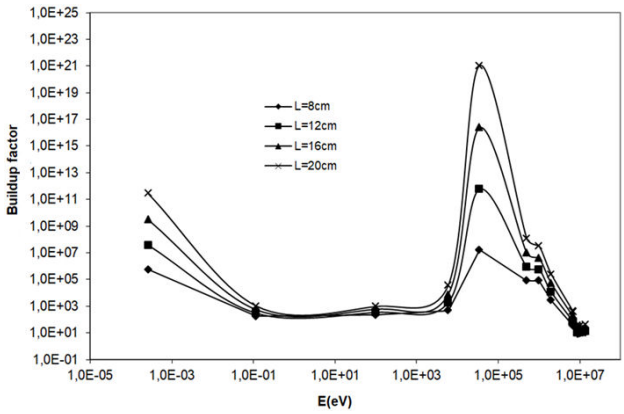

FIGURE 15. The buildup factor according to the energy of the incident neutrons for different lengths of the legs and for a square cross-section of 400 cm^2.

changes, increasing collisions and further slowing their energy. Additionally, the geometry of the duct extends the neutrons' path through the material, which increases the probability of absorption. Although aluminum has a low absorption capacity for fast neutrons, this effect becomes more pronounced as the distance traveled increases. Finally, multiple reflections due to the bents in the duct enhance interactions, further reducing the energy and flux of neutrons. These combined effects explain the attenuation of the neutron flux in the duct [19]. Figures 12 to 15 show the variations in the buildup factor according to the neutron energy for different lengths of the legs and different sides of the bent duct. We notice the existence of a positive peak at the energy level $E_0 = 35$ keV and that the buildup factor is greater when the length of the legs is greater and the sides of the duct are small. This can be explained by the shape of the cross sections and the diffusion and absorption probabilities. At the energy $E_0 = 35$ keV, the total cross-section and the probability of diffusion are very important while the probability of absorption is minimal; consequently, the flux at the outlet of the bent duct increases and that of Eq. (1) decreases; thus,

increasing the buildup factor [Eq. (2)] which becomes more and more important when the length of the legs increases and the side of the duct is small.

4. Conclusion

In a bent aluminum duct, high-energy neutrons lose energy through elastic scattering and increased collisions as their path changes. The duct's shape lengthens their journey, raising the chances of absorption. Additionally, reflections at the bents intensify neutron interactions, further reducing their energy. As a result, the number of neutrons moving through the duct decreases significantly. A new concept of the buildup factor is proposed and applied in this study. It can be concluded that this factor is greater than 1 and it increases when the length of the duct is great. It decreases when the energy of the incident neutrons is high.

1. K. Ueki and M. Kawai, Analyses and Development of Effective Compensation Shields in a Multilegged Duct Streaming System, *Radiation Protection*, **132** (2000) 281, https://doi.org/10.13182/NT00-A3144.
2. J. L. Kloosterman and J. E. Hoogenboom, Experiments and Calculations on Neutron Streaming Through Bent Ducts, *Journal of Nuclear Science and Technology*, **30** (1993) 611, https://doi.org/10.1080/18811248.1993.9734528.
3. M. Yamauchi *et al*, Experiment and Analyses for 14 MeV Neutron Streaming Through a Dogleg Duct, *Radiation Protection Dosimetry*, **116** (2005) 542, https://DOI:10.1093/rpd/nci236
4. K. Maki, Y. Morimoto and K. Shibata, Improvement of a simple Evaluation Method for Duct Streaming by Taking Account of the Deep Penetration Component, *Journal of Nuclear Science and Technology*, **38** (2001) 583, https://DOI:10.1080/18811248.2001.9715070
5. K. Hayashi, K. Yamada, K. Shin, F. Masukawa, Y. Naito, Duct-II and SHINE-II: simple design code for duct-streaming and skyshine, Japan Atomic Energy Research Institute Report, JAERI-M91-013, (1991).
6. C. M. Huddleston, J. C. LeDoux, in: R. Jaeger (Ed.), Springer-Verlag, *Engineering Compendium on Reactor Shielding*, **1** (1968) 488.
7. T. Nakamura, Y. Uwamino, *Radioisotopes*, **35** (1986) 51. https://DOI:10.3769/radioisotopes.35.2_51
8. K. Shin, Semiempirical Formula for Energy-Space Distributions of Streamed Neutrons and Gamma-Rays in Cylindrical Ducts, *J. Nucl. Sci. Technol.*, **25** (1988) 8. https://doi.org/10.1080/18811248.1988.9733551.
9. K. Shin, S. Selvi, T. Hyodo, Albedo Analytical. Method for Multi- Scattered Neutron Flux Calculation in Cavity, *J. Nucl. Sci. Technol*., **23** (1986) 949. https://doi.org/10.3327/jnst.23.949.
10. K. Tesch, The attenuation of the neutron dose equivalent in a labyrinth through an accelerator shield, Part. Accel. **12** (1982) 169. https://DOI:10.1016/0168-9002(93)91199-W
11. Y. Uwamino, T. Nakamura, T. Ohkubo, A. Hara, Measurement and calculation of neutron leakage from a medical electron accelerator, *Med. Phys*, **13** (1986) 374. https://DOI:10.1118/1.595879
12. H. Wijker, Simple approximation formula for gamma streaming through narrow air filled offset penetrations through reactor shields, Proceedings of the 3rd International Conference of Physics Problems and Reactor Shields, AERER- 5573 **3** (1969). Keuring van Electrotechnische Materialen, NV, Arnhem (Netherlands).
13. K. Goebel, G. R. Stevenson, J. T. Routti, H. G. Vogt, Evaluating dose rates due to neutron leakage through the access tunnels of the SPS, CERN Internal Report LAB II-RA/Note/75-10, (1975).
14. Z. Faik Ouahab *et al.*, New concept of the buildup factor in bent ducts, *Nuclear Instruments and Methods in Physics Research A (NIMA)*, **635** (2011) 78-81. https://doi.org/10.1016/j.nima.2011.02.014
15. D.B. Pelowitz, MCNPX User's Manual, Version 2.6.0, LA-CP-07-1473, (2008).
16. E. E. Morris, Moments Method Calculation of Buildup Factors for Point Isotropic Monoenergetic Gamma-Ray Sources at Depths than 20 Mean-Free-paths, *Nuc. Sci. Eng,* **50** (1973) 32, https://doi.org/10.13182/NSE73-A22585.
17. Y. Harima, An Approximation of Gamma Ray Buildup Factor by Modified Geometrical Progression, *Nuc. Sci. Eng, Technical Notes*, **83** (1982) 299, https://doi.org/10.13182/NSE83-A18222
18. E. Mauro, M. Silari, Attenuation of neutrons through ducts and labyrinths, *Nuclear Instruments and Methods in Physics Research Section A* **608** (2009) 28, https://doi.org/10.1016/j.nima.2009.06.045